Non-Covalent Functionalisation of Amorphous Carbon From D-Glucose as a Novel Catalyst for Renewable Fuels

Jidon Janaun, Ong Carrie, S.M Anisuzzaman, Duduku Krishnaiah*

Catalysis, Reaction Engineering & Drying Technology Research, Faculty of Engineering, Universiti Malaysia Sabah, 88400 Kota Kinabalu, Sabah, Malaysia

Abstract

In this paper, a renewable carbon catalyst was developed based on the non-functionalisation method. Three different pyrolysis temperatures at 400°C (SC400), 500°C (SC500) and 600°C (SC600) were used to prepare amorphous carbon. The non-covalent functionalisation was carried out by 1-pyrenesulfonic acid (1-PSA) in organic solvents such as ethanol, heptane and dimethylformamide (DMF), and characterised by total acidity, TGA, FT-IR, SEM-EDX, particle size, BET Porosity, and XRD. The total acidity was found to be 1.58 mmol/g for catalyst SC400. The functional groups –COOH, –OH, $–SO_3H$ and π-π stacking were detected. The amorphous carbon was stable until 500°C. The sulphur content was found to be 0.013mmol/g for SC400. This research approach focused on the direct interaction of carbonaceous support with pyrene moieties and terminal groups ($–SO_3H$) acting as catalytic acid sites that open a new way to be explored for performing liquid-phase heterogeneous acid-catalysed reactions.

Keywords: *Non-covalent functionalization, Amorphous carbon, sulfonation, surface morphology, D-Glucose carbon*

Introduction

The need for biodiesel as an alternative fuel diesel has increased nowadays as biodiesel is more environmentally friendly than petroleum-based diesel. Many researchers found ways to improve biodiesel production from vegetable oil and waste cooking oil. One of the important aspects of biodiesel production is the synthesis of catalysts for increasing the reaction rate and percentage of conversion [1]-[2]. It is produced by transesterification of triglycerides with methanol in the presence of acid or base heterogeneous catalysts. The solid acid catalysts included sulphated catalysts. Incorporating sulphate ions showed a strong influence on biodiesel production [3]-[5].

Carbon materials constitute a very flexible set of supports for elaborating robust advanced heterogeneous catalysts and their increasing importance in catalytic processes is now widely recognised in biodiesel production [1], [6-7]. Covalent functionalisation is a chemical functionalisation and associated with a hybridisation change from sp_2 to sp_3 and a simultaneous loss of the pi-conjugation system on the graphene layer. The non-covalent functionalisation is a physical functionalisation by aromatic compounds, surfactants, and polymers, employing π-π stacking or hydrophobic interactions. Carbon material with its unique electronic, thermal, and mechanical properties, such as amorphous carbon and carbon nanotubes exhibits remarkable stability due to its hydrophobic nature in the presence of polar solvents. Such unique behaviour emerges from the hydrophobic nature of multi-wall carbon nanotubes or amorphous carbon's surface because of their unique π-conjugated system favoring the aromatic-based reagent. The advantages of producing non-covalent functionalisation instead of covalent functionalisation are due to the functional groups' attachment. This method offers the possibility of attachment to graphene without disturbing the electronic network and does not disrupt the extended π-conjugate on the graphene surface. This means that in the acid catalytic reaction, the amorphous carbon can be attached with $–SO_3H$ group by non-covalent functionalisation. In order to improve the graphene solubility in common solvents and avoid stacking, the non-covalent functionalisation with the different organic compounds is essential [2], [8].

Pi(π) stacking implies an attractive non-covalent interaction between aromatic rings. Sigma and pi atomic charges, relative orientations, and van der Waals interactions qualitatively determine the electrostatics which is dominant in substituent effects. The electron-withdrawing groups reduce the negative quadrupole of the aromatic ring and thereby favour parallel displacement and sandwich conformations. However, the electron-donating groups increase the interaction strength in a T-shaped configuration with proper geometry [9].

Non-covalent functionalised the carbon solid through π-π stacking with non-polar solvent as a stabiliser to produce immobilised acidic catalytic active centres. The functionalisation depends on the type of solvent used in the sulfonation process. The formation of non-covalent nonspecific functionalisation and solubilities of multi-walled carbon nanotubes (MWCNTs) was found to be effective in the organic solvent [10].

The amorphous carbon can be prepared by carbonisation through pyrolysis. Carbonisation involves the thermal decomposition of carbonaceous material, eliminating non-carbon species producing a fixed carbon mass and rudimentary pore structure. The higher the carbonisation temperature, the higher the specific surface area of the char. However, the catalytic activity of esterification is independent of the surface area and depends on acid density. The basic microstructure of the char with microporosity was formed around 500°C. If the carbonisation temperature is not more than 450°C, some of the glucose does

*Corresponding author.
E-mail address : krishna@ums.edu.my

not transform into char, whereas, if the process is carried out at a temperature higher than 550°C, the heat decelerates the activation process [11].

A way to increase the $–SOH_3$ group in non-covalent functionalisation was proposed [12]. In this work, electrodes were prepared using single-walled carbon nanotubes non-covalently functionalised with 1,3,6,8-pyrenetetrasulfonate or 1-pyrenesulfonate and immobilised together with enzyme lactase. This method enables the immobilisation of the controlled number of sulfonate groups. However, the results obtained from these experiments are different than reported [13]. The pyrene functionalised single-wall carbon nanotube (SWCNT) electrodes are reproducible and show significantly higher catalytic current with 1,3,6,8-pyrenetetrasulfonate acid.

The interaction is from the negatively charged functional groups and electron clouds of the π systems which exhibit an attractive interaction. This interaction is predominated by dispersion interaction when both π systems possess very similar electron densities. When one of the systems is electron-rich, and another electron is electron-deficient, the resulting complexes are bound by induction interactions as is the case when the negative charge gets transferred from benzene [12]. The 1-PSA molecules on the graphene layers' surface act as electron-withdrawing groups resulting in an electron transfer from the modified graphene nanosheets surface to the 1-PSA molecules [14]. The non-covalent modification of CNTs surface through π–π stacking with 1-pyrenesulfonic acid (PSA) was reported [15]. The attractive interaction between the pyrene moieties and the CNTs surface binds them together. In this study, a renewable carbon catalyst was developed based on non- functionalisation method using glucose as a carbon source.

Materials and Methods

Materials

Glucose (99%) was obtained from SYSTERM ChemAR as the raw material for amorphous carbon by the pyrolysis process. 1-pyrenesulfonic acid hydrate was purchased from SIGMA-ALDRICH (>97% HPLC). Besides that, nitrogen gas (98%) was purchased from a local supplier for the pyrolysis process to purge out all the oxygen and moisture. The solvents used in the sonication process were ethanol (96%) from SYSTERM ChemAR, N, N-dimethylformamide DMF (99.8%) from J T Baker, and heptane (99%) from R&M Chemicals Company.

Preparation of catalyst

The glucose was subjected to pyrolysis at 400, 500, and 600°C in a tubular furnace. The nitrogen was used to purge out all the oxygen gas and moisture for 30 minutes at a flow rate of 100 ml/min. The time taken for the pyrolysis for these three different temperatures was 4 hours. After four hours of pyrolysis, the flowing nitrogen gas was stopped out of the beaker that contained water before it turned off to avoid the backflow of water into the tubular furnace. The sample inside the tube furnace was taken out. The char was reduced to powder and sieved to below 2 mm before analysis. The samples were stored in a desiccator for further analysis.

Liquid sulfonation

1-pyrenesulfonic acid hydrate was heated in an oven for three hours at 105°C to remove the hydrate. The non-covalent functionalisation of amorphous carbon was carried out by mixing the glucose amorphous carbon (1 g) with 1-pyrenesulfonic acid (100 mg) in ethanol (100 mL). The resulting mixture was sonicated at room temperature in the fume hood allowing the vapours released to the atmosphere for 30 minutes. After bath-sonication, the solvent was filtered with filter paper. Then the catalyst was dried under vacuum at 40°C for 24 hours [16]. This procedure was repeated using heptane, N, N-DMF [15] solvents.

Post Sulfonation

The samples were washed with hot distilled water repeatedly until the pH becomes neutral, and the sulphate ion was not detected. The samples were dried in an oven at 110°C [17]. All the samples were kept in a desiccator at room temperature until it is further used. Another test by a precipitate of barium sulfate was used to detect the sulfate ion. 2 mL of HCl was then added into the sample and washed with water. The sample was then heated to boiling point while stirring gently and 0.1 M of barium dichloride was added slowly into it. If there is no formation of white precipitate means that the sulfate ion does not exist.

Total Acidity Analysis

The samples were tested through their chemical and physical properties. Catalyst characterisation was carried out by measuring its total acidity using acid-base back titration. For the back titration, 0.008 M of NaOH and 0.02 M of HCl reagents were used.

TGA Analysis

The determination of thermal stability was carried out using thermal gravimetric analysis (TGA) with the Perkin Elmer model TGA6. TGA is the determination of the weight change as a function of temperature under a controlled atmosphere. The sample was preheated in a flowing inert atmosphere (10°C/min) at 400°C with 100 ml/min a flow rate. When the sample equilibrated at the specified temperature, the furnace was switched from inert gas. After that, the desorption of the adsorbed base was done by switching back to an inert atmosphere. The temperature was increased at the rate of 10°C/min to remove base molecules. The process was repeated for all samples [18].

FTIR Analysis

The functional group was determined by using Fourier Transform Infrared Spectrometry (FTIR). The FTIR resulting spectrum indicates the molecular absorption and transmission, creating a molecular

fingerprint of the test sample. Complete temperature series of the non-covalent functionalisation char was scanned in the mid-infrared region from 650-4000 cm^{-1} by using the software. The spectrum was analysed to determine the functional groups for respective chars.

SEM Morphology

The surface morphology analysis was determined by using a Scanning Electron Microscope (SEM). The morphology of chars from different temperatures (400, 500 and 600°C) and different solvents (heptane, ethanol, and DMF) was determined. All the samples are solid and sufficient size to fit into the microscope chamber. The maximum size in horizontal dimensions is about 10 cm, and the vertical dimension is about 40 mm. The samples are stable in the vacuum at the order of 10^{-5} or 10^{-6} torr. Energy-dispersive X-ray microanalysis (EDX) is to determine the composition of the features in the SEM image. Its characterisation capabilities are due to each element that exhibits a unique atomic structure allowing X-rays that are characteristic of an element's atomic structure to be identified uniquely from one another.

XRD Analysis

The XRD is one of the most commonly used techniques for the crystalline phase identification. In this technique, the catalyst sample was irradiated with the X-ray of a known wavelength (λ). Accordingly, X-rays are reflected by atomic layers with interplanar spacing (d) at a certain angle of incidence and reflection, which is well known as Bragg angle (θ) [19]. The particle size distribution by volume was measured using a Malvern Zetasizer Nano series with water as a dispersant (refractive index = 1.330).

Surface Area and Porosity Determination

The Brunauer Emmet Teller (BET) method was used for calculating the total surface area. Each sample surface area was measured based on the BET multipoint method using Automatic Mercury Porosimeter (PASCAL 400) [20].

Result and Discussion

Total Acidity

The data of total acidity is shown in Figure 1. It shows that the catalysts' total acidity is increased from 1.587 mmol/g to 1.613 mmol/g when the temperature is increased from 400 to 500°C. However, at 600°C, the acidity is decreased to 1.273 mmol/g. The overall trend of the total acidity shows a decreasing magnitude. This may be due to the higher carbonisation temperature and the higher surface area of the catalyst support. However, if the carbonisation temperature is too high, the structure of the catalyst support changes. This decrease in total acidity might be attributed to the lower amount of polycyclic aromatic carbon being functionalised in the catalyst at a higher temperature at 600°C. The pyrolysis was carried out in the temperature range 250-650°C. The higher temperature would adversely effect on the formation of the $–SO_3H$ group during the sulfonation process due to the formation of rigid carbon material. Besides, this results in the low acid density and inability of certain polar molecules to reach the $–SO_3H$ groups. Thus, the high-temperature pyrolysis process can result in a limited catalyst. However, the lower pyrolysis temperatures at the longer time favoured the thermal-resistant carbon material, which can result in the carbon that is more prone to be sulfonated. The highest activity of the synthesised catalyst was found to be at 400°C, as shown in Figure 1.

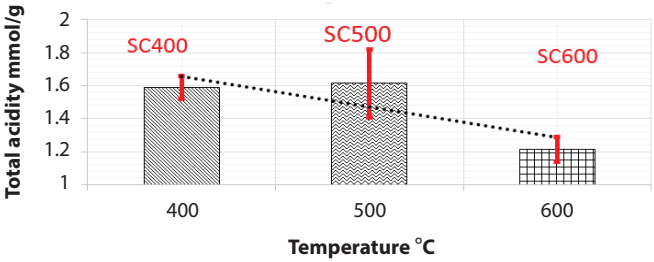

Figure 1 Effect of temperature on total acidity

Particle Size Distribution and Functional Groups

Figure 2 shows the particle size distribution of carbon-based catalysts. The mean particle size was based on a volume-weighted mean. The mean particle sizes of samples SC400, SC500, and SC600 were 147.2 nm, 112.9 nm, and 100.6 nm. From the size distribution, the higher the carbonisation temperature, the smaller the particle size. By increasing the activation temperature, the carbon structure becomes ordered to a certain extent, but not to the extent of completely ordered graphite carbon structure. Therefore, an ordered porous carbon structure was formed by increasing the activation temperature.

The FT-IR spectrum is shown in Figure 3 and Table 1. All of the spectra contain peaks attribute to aromatic ring modes around 1600 cm^{-1}. C=C stretching can be identified at the range wavenumber of 1620-1680 cm^{-1} [21]. Moreover, peaks attribute to C-O-C asymmetric stretching for all sulfonated char catalysts can be seen at about 1130-1150 cm^{-1} [18]. The $-SO_3H$ exhibits a peak at 1000-1032 cm^{-1} attributed to the symmetric S=O stretching [22], as well as a peak at 1743 cm^{-1} attributable to the presence of $–SO_3H$ groups, thereby confirming the incorporation of sulfonic groups onto carbon matrix after the sulfonation process [23]. All the three spectra exhibited similar peaks characteristic of $–SO_3H$ groups at 1743 cm^{-1}; however, SC-400 is slightly more intense than SC-500 and SC-600. This shows the reduction of catalysts' total acidity by increasing the activation temperature of the support due to the constitution of large carbon sheets and essentially a more ordered structure. The three sulfonated char catalysts show the peaks around 1215 cm^{-1} can be assigned to an aromatic acidic group (Ar-OH stretch) mainly due to oxidation during the carbonisation and the peak around 1700 cm^{-1} attribute to C=O, which assigned to carboxylic groups [24]. However, it can be seen that there is a peak of about 3400 $cm^{-1,}$ which is known as OH stretching at 3200-3700 cm^{-1} [25].

Table 1 Characteristics of FTIR spectrum

Wave number, cm^{-1}	Group attributed
841	C-H wagging vibration
845	Strong ring deformation
1000 – 1032	S=O stretching symmetric
1130 – 1150	C-O-C asymmetric stretching
1215	Aromatic acidic group
1550	Ring stretching peak
1620-1680	C=C stretching
1700	C=O carboxylic groups
1743	Presence of -SO_3H group
3200 – 3700	OH stretching

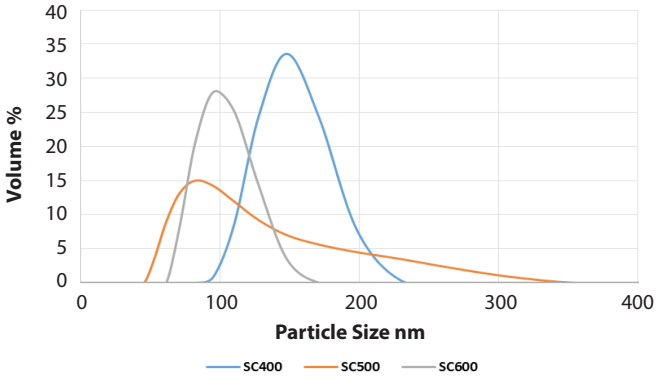

Figure 2 Particle size distributions of SC400, SC500, and SC600

As shown in Figure 3, the peaks for all catalysts at 1600 cm^{-1} are significant. This FT-IR spectrum showed a characteristic peak of pyrene such as a strong ring deformation peak at 845 cm^{-1} and a ring stretching peak at 1550 cm^{-1} indicating successful incorporation of pyrene into the amorphous carbon [26]. This confirms that non-covalent interaction occurs between the sulfonated pyrene group (–SO_3H) and the amorphous carbon sheet's carboxylate groups. The FT-IR spectrum of pyrene shows a strong peak at 841 cm^{-1} which is attributed to C-H wagging vibration. These bands of amorphous carbon incubated with pyrene were caused by the strong *π-π* stacking interaction in the pyrene-amorphous carbon complex [27].

Surface Morphology

Figure 4a, Figure 4b, and Figure 4c show SEM images of physical change in SC600 and SC500 compared to SC400. As a result of the high-temperature pyrolysis process, the porosity in SC500 is higher compared to SC400. However, for SC600, by increasing the activation temperature, the number of C-C bonds in the carbon lattice increases. The degree to which the pores collapse decreased, as shown in Figure 4c SEM image. This is attributed to the lower total acidity of the SC600 compared to SC400 and SC500 due to the destroyed and the collapsed walls, which are appeared as flakes [28].

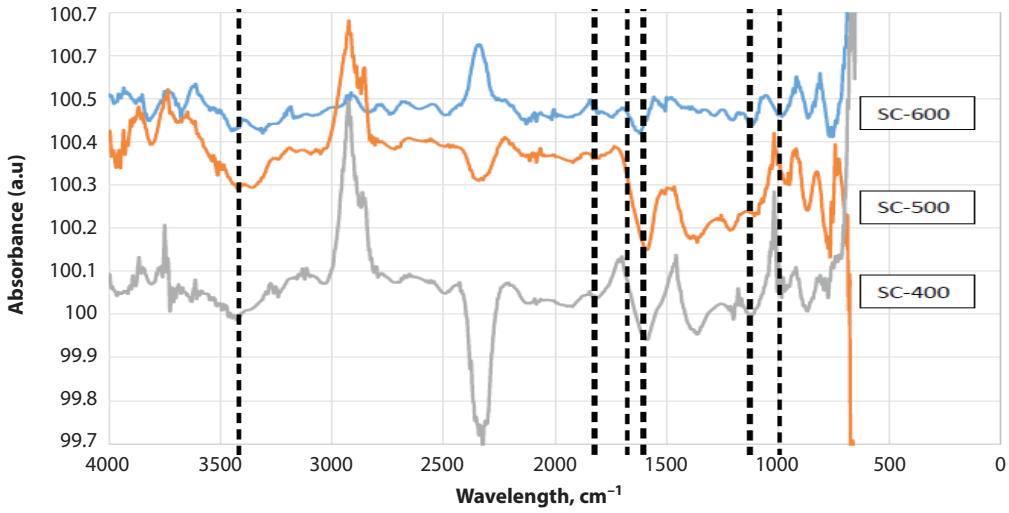

Figure 3 FT-IR spectra of char and the carbon-based catalyst

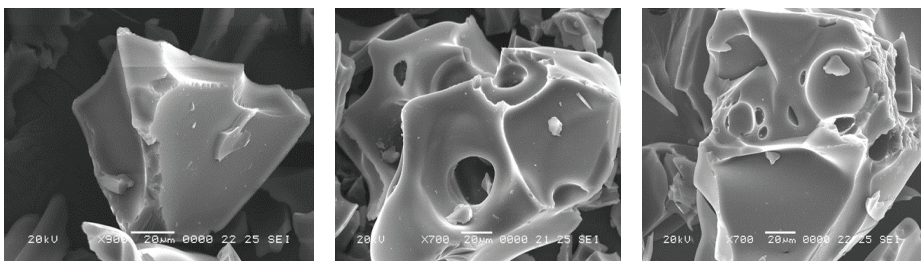

Figure 4 SEM images of SC400, a) SC500, b) SC600, c) with the magnification of 700

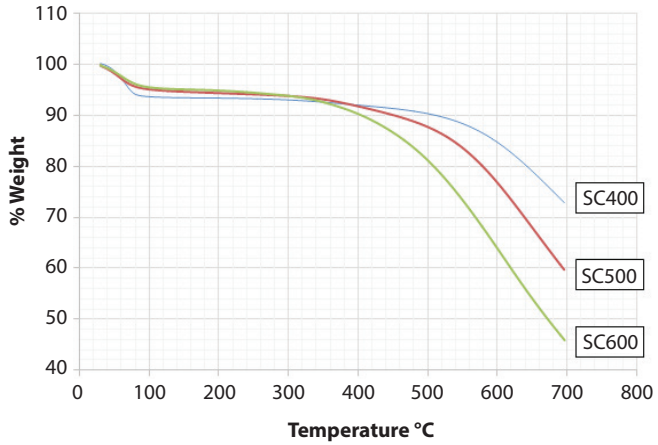

Figure 5 Thermo-gravimetric analysis (TGA) of SC400, SC500, and SC600 under nitrogen

Thermal Stability

The thermal-gravimetric analysis (TGA) of the carbon-based catalyst under nitrogen is shown in Figure 5. The weight loss is about 5% at 100°C, which is mainly due to the loss of the amount of water adsorbed. The non-covalent binding decomposition temperature is between 350-600°C. It also proves that the shift of characteristic of non-covalent functionalisation between hexagonal rings and pyrene molecules in TGA, which is decomposed from 300°C [29]. The TGA profile is observed upon π-π bonding decomposition gives way to stepwise weight loss pattern around 325°C. This phenomenon was observed with non-covalent functionalisation sulfonated carbon catalyst wherein guest molecules sustain and stabilise the open structure. From the TGA analysis, it was found that SC600 at higher carbonisation temperature showed less significant weight loss compared to SC500 and SC400. This may due to the gradual desorption of SC600 compared to SC400 and SC500, which has low acidity 1.2 mmol/g.

Surface Element Analysis

The chemical composition of the carbon-based catalyst was analysed using an elemental analysis method. The ratio of O:C is higher in SC600 compared to SC400 and SC500. The results of element analysis are shown in Table 2. It shows that the decrease in the O:C ratio with the increasing activation temperature. Increasing the activation temperature causes the evaporation of an increasing number of heteroatoms from the carbon rings resulting in more graphite-like structure and more ordering [30]. On the other hand, the element analysis shows only the SC400 consists of the sulphur element, which is 0.0012 mol while SC500 and SC600 do not possess sulfur element.

XRD Spectroscopy

In this work, the sulfonated carbon-based catalyst samples have shown disorder towards a specific direction to its carbon sheets which is known as turbostratic. This is due to the typical XRD patterns of these materials are either considerably broad or absent compared to that of graphite structures [31]. However,

Table 2 Element analysis of different temperature sulfonated catalyst

Catalyst	Temperature, [°C]	Mol			$-SO_3H$ [mmol/g]	Mol ratio to Carbon	
		C	O	S		O:C	S:C
SC400	400	7.19	0.85	0.0012	0.013	0.118	$1.7x10^{-4}$
SC500	500	7.26	0.80	0.00	0.00	0.11	0.00
SC600	600	7.92	0.30	0.00	0.00	0.04	0.00

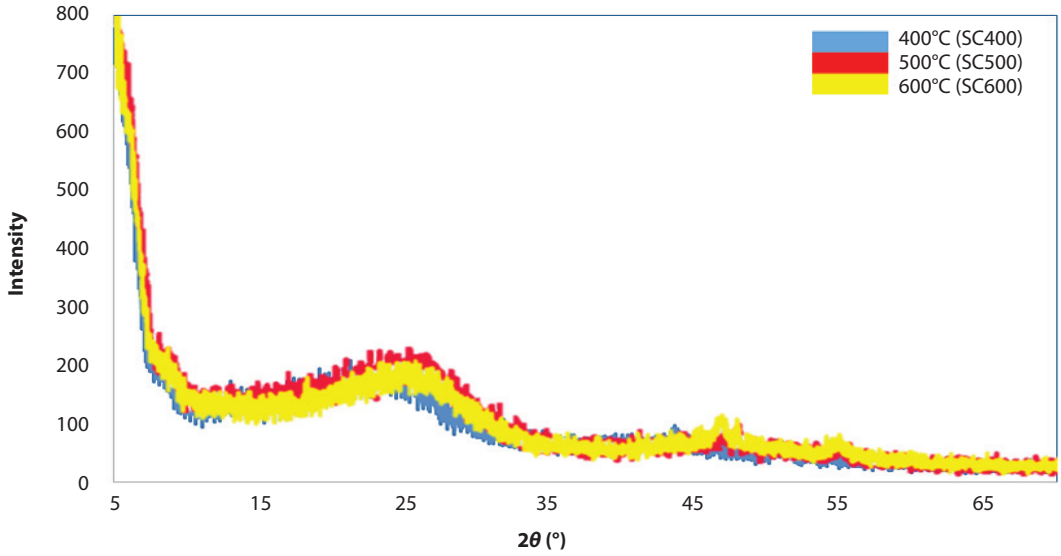

Figure 6 XRD Pattern of catalyst prepared from char carbonized at 400°C (SC400), 500°C (SC500), 600°C (SC500)

the development of an increasing ordered structure within the carbon network is determined by the presence of definitive narrow peaks of graphite structure in the XRD patterns compared to the broader ones [32].

Figures 6 shows the XRD patterns for carbonised glucose with different temperatures. All the XRD patterns exhibit similar diffraction peaks around 2θ=10-30° attributable to amorphous carbon composed of aromatic carbon sheets oriented in a considerably random fashion. In the case of glucose, carbonised at 600°C, Figure 6 clearly shows a diffraction peak at 2θ = 35-50°C appears broader and weaker compared to SC400 and SC500. This diffraction indicates the presence of more graphite likes structure at higher temperatures [33].

Surface Area and Porosity

The porosity of the carbon-based catalyst is shown in Table 3. It shows that the particles are mesoporous characteristics with an average pore size ranging from 40 nm-1694 nm while the surface area is ranging from 4-7 m^2/g. Increasing the carbonization temperature from 400°C to 600°C of the carbon char, the pore diameter increased considerably. Sulfonated char prepared at carbonisation temperature at 400°C results in a 28% reduction in surface area compared to 600°C. Simultaneously, the carbonisation temperature at 500°C did not much reduce in surface area compared to 600°C, which is only 9.17%. However, with the increasing carbonisation temperature, carbon material becomes harder, and the flexibility of polycyclic aromatic carbon decreased through-plane growth and carbon sheet stacking [34].

Table 3 Surface area, pore diameter and porosity of three different pyrolysis temperature sulfonated catalyst

Catalysts	Surface area [m^2/g]	Pore diameter [nm]	Total porosity [%]
SC400	4	41.70	5.22
SC500	6	247.85	8.25
SC600	7	1694.22	8.79

Effect of Temperature on Surface Area and Total Acidity

Three sulfonated catalysts made from three different pyrolysis temperatures (400, 500, and 600°C) were studied for their total acidity, surface area, and porosity. Figure 7 shows the increased surface area of the catalyst at higher carbonisation temperature. Furthermore, the activated support at the lowest carbonisation temperature showed a considerable reduction in the surface area. Nevertheless, the percentage of the surface area was increased considerably for sulfonated catalysts at higher temperature i.e. 500°C and 600°C. Therefore, in this study, it was observed that the surface area and porosity of the prepared catalyst are important factors on the total acidity. However, increasing the pyrolysis temperature would cause more C-H bonds ruptured through completing the carbonisation of the support [35]. The polycyclic

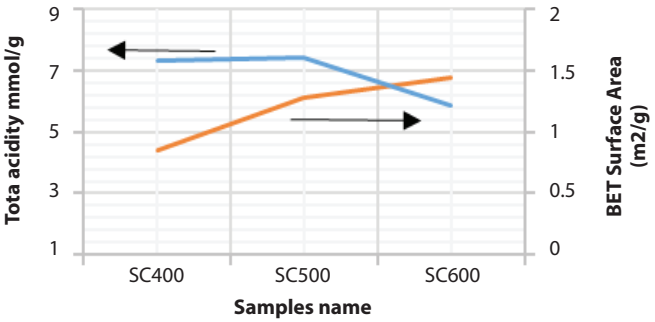

Figure 7 Effect of temperature on surface area and total acidity of amorphous carbon functionalised

aromatic carbon in this sample is thus expected to be less flexible. Therefore, the large inflexible polycyclic aromatic carbon in rigid carbon materials can be sulfonated with sulfonate ion.

Effect of Solvent on Non-Covalent Functionalisation

Amorphous carbon is a natural and inexpensive source for large scale production of graphene sheets. However, the π-π stacking between graphene sheets results in the formation of multilayers. Pristine graphene sheets are hydrophobic; hence they cannot dissolve in polar solvents. Thus, to make graphene soluble in common solvents, and thereby avoiding stacking, the non-covalent functionalisation with a different organic solvent is essential such as heptane, ethanol, and DMF [36]. However, organic solvents can be divided into polar or non-polar solvents. The successful non-covalent functionalisation of graphene was suspended in the non-polar solvent with non-polar pyrene derivatives. Interactions between amorphous carbon and noncharged non-polar molecules in non-polar media to a higher extent, rely on non-covalent functionalisation. The non-polar pyrenes are designed primarily to provide the interaction in the non-polar aromatic solvent that can be non-covalently functionalised by neutral pyrene derivatives [9]. In this study, based on the total acidity, it is obvious that heptane led to the highest adsorption of 1-pyrenesulfonic acid onto these solids among the solvents used. This is because of the heptane, which is widely applied as a non-polar solvent compared to ethanol and DMF, which consist of polar characteristics. The surface area and total acid increase with the increasing pyrolysis temperature, resulting in larger pore size, which allows the sulfonic acid groups to be more easily incorporated into the carbon matrix by diffusion [22]. Therefore, the chars with lower pyrolysis temperature preserved the intrinsic properties of graphite carbon via π-π interaction.

Comparison between Non-Covalent Functionalised Carbon-Based Catalyst with Sugar Catalyst

The comparison between the non-covalent sulfonated catalyst with the pyrolysis temperature 400°C using 1-pyrenesulfonic acid as a reactant and sugar catalyst derived from D-glucose is shown in Table 4. Table 4 shows that the total acidity of sugar catalyst is higher than the SC400. However, the sugar catalyst's surface area did not exceed 1 m^2/g despite supported on porous media. From the thermo-gravimetric (TGA) of carbon-based catalysts under

Table 4 Comparison between non-covalent functionalised carbon-based catalyst with sugar catalyst

Characteristics	**SC400**	**Sugar catalyst**
Type of functionalization	Non-covalent	Covalent
Total acidity, [mmol/g]	1.586	3.89
Surface area, [m^2/g]	4.41	<1
Porosity [%]	5.22	-
Crystallinity	Amorphous (disordered) and crystalline (ordered)	Amorphous
Thermal stability (decomposition of functional groups)	500°C	247°C
Functional groups	π-π stacking with pyrene group, -OH and -COOH	sp^3 bonding with –SO^3H group, -OH and -COOH

nitrogen, sugar catalyst showed the decomposing trend at around 247°C. This is contrary to SC400, which is decomposing at around 500°C, where it is thermally more stable than sugar catalyst. This can be explained by the analysis of the elemental composition where sugar catalyst consists of 0.07 ratio of S:C while SC400 consists of a 1.7 x 10^{-4} ratio of S: C. SC400 has a relatively higher amount of carbon compared to sugar catalyst but lower total acidity compared to sugar catalyst. Although non-covalent functionalisation-based acid catalyst (SC400) consists of lower total acidity compared to covalent functionalisation (sugar), the non-covalent (π-π stacking) functionalisation route is simple to handle and non-destructive, thereby avoiding deterioration of the outer electronic surface of the MWCNT and C/C composites. Since covalent functionalisation of the larger planar unsaturated carbon system introduces sp^3sites and changes the permanent electronic properties. In contrast, the non-covalent has the advantage of preserving the amorphous carbon's structural and electronic integrity.

Conclusion

In this work, three types of non-covalent functionalisation of carbon at three different pyrolysis temperatures at 400, 500, and 600°C were studied. This is confirmed by the shift 1550-1600 cm^{-1} in the FTIR spectrum where 1-PSA molecules on the amorphous carbon act as the electron-withdrawing groups resulting in the electron transfer from amorphous carbon to 1-PSA form a π-π stacking. Based on the BET analysis, the results suggest that the total acidity of the catalyst, surface area and porosity of the non-covalent sulfonated catalyst are important factors. From the elemental analysis by EDX, only SC400 consists of the sulfur element while S500 and S600 do not possess any sulfur element on the surface of the catalyst. Acid back titration also confirmed that there is total acidity inside the SC400 catalyst (1.586 ± 0.356 mmol/g). Besides that, TGA and DTA analysis show that the non-covalent functionalisation catalyst decomposed at 500°C is highly stable compared to the sugar catalyst at 247°C. Future studies include transesterification of vegetable oil with methanol using the catalyst prepared and process optimisation with response surface methodology.

Acknowledgement

Authors would like to express sincere gratitude to the centre for research and innovation, Universiti Malaysia Sabah for providing necessary support for this project.

References

[1] M. Hara, "Biodiesel Production by Amorphous Carbon Bearing SO3H, COOH and Phenolic OH Groups, a Solid Bronsted Acid Catalyst", *Topics in Catalysis*, 53, pp. 805-810, 2010. Doi.10.1007/s11244-010-9458-z.

[2] B. Fielder, F. H Gojny, M.H.G Wichmann, M.C.M Nolte & K. Schuttle, "Fundamental Aspects of Nano-reinforced Composites", *Composites Science and Technology,* 66, pp. 3115-125, 2006. Doi:10.1016/j.compscitech.2005.01.014.

[3] J.A. Melero, L.F Bautista, G. Morales, J. Iglesias, & R. Sánchez-vázquez, "Biodiesel production from crude palm oil using sulfonic acid-modified mesostructured catalysts", *Chemical Engineering Journal*, 161, pp. 323-331, 2010. Doi.10.1016/j.cej.2009.12.037

[4] A. Patel, V. Brahmkhatri & N. Singh, "Biodiesel production by esterification of free fatty acid over sulfated zirconia", *Renewable Energy*, 51, pp.227-233, 2013. Doi.10.1016/j.renene.2012.09.040.

[5] D. Rattanaphra, A.P Harvey, A. Thanapimmetha & P. Srinophakun, "Simultaneous transesterification and esterification for biodiesel production with and without a sulphated zirconia catalyst", *Fuel,* 97, pp. 467-475, 2012. Doi.10.1016/j.fuel.2012.01.031.

[6] R.K Zhang , K. Chen , X. Huang, L. Wohlschlager, H. Renata & F.H Arnold , "Enzymatic assembly of carbon-carbon bonds via iron-catalysed sp3 C-H functionalisation", *Nature*, 565 , 7737, pp. 67-72, 2019. Doi:10.1038/s41586-018-0808-5

[7] H.I. Abdu , K. Eid, A.M Abdullah & X. Lu, "Data on the synthesis and characterisations of carboxylates carbon-based catalyst from eucalyptus as efficient and reusable catalysts for hydrolysis of eucalyptus", *Data Brief*, 30, p. 105520, 2020. Doi:10.1016/j.dib.2020.105520

[8] X. Yan Liu , M. Huang, H.L Ma, Z.Q Zhang, J.M Gao, Y. L Zhu, X. Jin Han & X. Y Guo, "Preparation of a carbon-based solid acid catalyst by sulfonating activated carbon in a chemical reduction process", *Molecules*, 15, 10, pp. 7188-196, 2010. Doi:10.3390/molecules15107188.

[9] V. Geogakilas, M. Otyepka, A.B. Bourlinos, V. Chandra, N. Kim, K.C. Kemp, P. Hobza, R. Zboril & K.S Kim, "Functionalisation of Graphene: Covalent and Non-Covalent Approaches, Derivatives and Applications", *Chemical Review*, 112, pp. 6165-214, 2012. Doi.10.1021/cr3000412.

[10] X. Lixin, Y. Zhibin, C. Qingzhou, & G. Zhiyong, "Noncovalent Nonspecific Functionalization and Solubilization of Multi-Walled Carbon Nanotubes at High Concentration

with a Hyperbranched Polyethylene", *Macromolecular Chemistry and Physics,* 210, pp. 2194-202, 2009. Doi.10.1002/macp.200900460.

[11] M. Kitano, K. Arai, A. Kodama, T. Kousaka, K. Nakajima, S. Hayashi, & M. Hara, "Preparation a Sulfonated Porous Carbon Catalyst with High Specific Surface Area" *Catalysis Letters,* 131, pp. 242-249, 2009. Doi.10.1007/s10562-009-0062-4.

[12] M. Jonsson-Niedziolka, K. Szot, J. Rogalski & M. Opallow, "Pyrene Sulfonate Functionalized Single-Walled Carbon Nanotubes for Mediatorless Dioxygen Bioelectrocatalysis", *Electrochemistry Communications*, 11, pp. 1042-1044, 2009. Doi.10.1016/j.elecom.2009.03.007.

[13] H. Yang, Y. Hernandez, A. Schlierf, A.Felten, A. Eckmann, A.Johal, P. Louette, J.J. Pireaux, X. Feng, K. Muellen, V. Palermo & A. Casiraghi, "Simple Method For Graphene Production Based on Exfoliation of Graphite in Water Using 1-Pyrenesulfonic Acid Sodium Salt", *Carbon, 35*, pp. 357-365, *2013.* Doi.10.1016/j.carbon.2012.11.022.

[14] J.H. Jang, D. Rangappa, Y-U. Kwon, & I. Honma, "Direct Preparation of 1-PSA Modified Graphene Nanosheets by Supercritical Fluidic Exfoliation and Its Electrochemical Properties", *Journal of Material Chemistry,* 10, pp. 3253-3496, 2011. Doi.10.1039/C1JM90012A.

[15] G.J. Souquet, H. Plaisantin, J. Thebault, F. Jerome, J. Barrault, J.M. Tatibouet, & S. Valange, "Non-Covalently Functionalised Multiwalled Carbon Nanotubes as Novel Active and Reusable Acid Catalyst", 2010. [Online] Retrieved from http://www.researchgate.net/publication/266586539.

[16] D. Rangappa, J-H. Jang & I. Honma, Supercritical Fluid Processing of Graphene and Graphene Oxide. Croatia, *INTECH*, 2011. [Online] Retrieved from http://cdn.intechopen.com/pdfs/19777.pdf

[17] J.A. Janaun, T.J. Mey, A. Bono & D. Krishnaiah, "Preparation and Characterisation of Sugar-Based Catalyst on Various Supports", *Bulletin Chemical Reaction Engineering and Catalysis*, 12, pp. 41-48. 2017. Doi.10.9767/bcrec.12.1.478.41-48.

[18] J.M Blaine, "Thermal Analysis Application Brief TGA Evaluation of Zeolite Catalyst", Retrieved from *TA Instruments Thermal Analysis & Rheology*, 2010. [Online] Retrieved from www.tainstruments.com/library_download.aspx?file=TA231.PDF.

[19] M. Birkholz, C. Genzel, & T. Jung, "X-Ray Diffraction Study on Residual Stress and Preferred Orientation in Thin Titanium Films Subjected to A High Ion Flux During Deposition", *Journal of Applied Physics,* 96, p. 7202, 2004. Doi.org/10.1063/1.1814413.

[20] A. Trunschke, "Surface Area and Pore Size Determination", *Modern Methods in Heterogeneous Catalysis Research*, Kluwer Academic Publisher, Dordrecht, 2004.

[21] K.R. Sharma, B.W. Jan, L.B. Vicki, L. Xuehao, W.C. Geoffrey & H.R. Mohammad, "Characterisation of Chars from Pyrolysis of Lignin", *Fuel,* 83, pp. 1469-482, 2004. Doi.10.1016/j.fuel.2003.11.015.

[22] W. Zhou, Y. Makoto, K. Hidetoshi, & O. Ken-ichi, "Carbon Molecular Sieve Membranes Derived from Phenolic Resin with a Pendant Sulfonic Acid Group", *Industrial & Engineering Chemistry Research,* 40, p. 22, 2001. Doi.10.1021/ie010402v.

[23] R. Xing, Y. Liu, Y. Wang, L. Chen, H. Wu, Y. Jiang, M. He & P. Wu, "Active Solid Acid Catalysts Prepared by Sulfonation of Carbonisation-Controlled Mesoporous Carbon Materials", *Microporous and Mesoporous Materials,* 105, pp. 41-48, 2007. Doi.10.1016/j.micromeso.2007.06.043.

[24] M.H. Zong, Z.Q. Duan, W.Y. Lou, T.J. Smith & H. Wu, "Preparation of a sugar catalyst and its use for highly efficient production of biodiesel", *Green Chemistry, 9*, pp. 434-437, 2007. Doi.10.1039/B615447F.

[25] X. Mo, L. Edgar, L. Changqing, L. Yijun & G. James "A Novel Sulfonated Carbon Composite Solid Acid Catalyst for Biodiesel Synthesis", *Catalysis Letters,* 123, pp. 1-6, 2008. Doi.10.1007/s10562-008-9456-y.

[26] X. Lou, R.Daussin, S. Cuenot, A. Duwez, C.Pagnoulle, C, Detrembleur, C.Bailly & R. Jérôme, "Synthesis of Pyrene-Containing Polymers and Noncovalent Sidewall Functionalization of Multiwalled Carbon Nanotubes" *Chemical Materials,* 16, 21, 4005-011, 2004. Doi.10.1021/cm0492585.

[27] Y. Zhang, S. Yuan, W. Zhou, J. Xu & Y. Li, "Spectroscopic Evidence and Molecular Simulation Investigation of the Interaction Between Pyrene Molecules and Carbon Nanotubes", *Journal of Nanoscience and Nanotechnology*, 7, 7, pp. 2366-2375, 2007. Doi.10.1166/jnn.2007.412.

[28] R. Xing, Y. Liu, Y. Wang & L. Chen, "Active solid acid catalysts prepared by sulfonation of carbonisation-controlled mesoporous carbon materials", *Microporous and Mesoporous Materials*, 105, 1-2, pp 41-48, 2007. Doi.10.1016/j.micromeso.2007.06.043.

[29] C. Valente, E. Choi, M.E. Belowich, C.J. Doonan, Q. Li, T.B. Gasa, Y. Youssry, M. Omar & J.F. Stoddart, "Metal-organic frameworks with designed chiral recognition sites", *Chemical Communications,* 46, pp. 4911-4913, 2010. Doi.10.1039/C0CC00997K.

[30] D. Lee, S.S. Ho, J. Wang, J.S Hwan, P.K. Hyun, K.B. Hyun, H.S. Hyung & S. Jeon, "Enhanced Mechanical Properties of Epoxy Nanocomposites by Mixing Non-covalently Functionalised Boron Nitride Nanoflakes", *Small,* 12, pp. 2602-10, 2013. Doi.10.1002/smll.201203214.

[31] J. Lehmann & J. Stephen, *Biochar for Environmental Management*, [Online] Retrieved from https://www.biochar-international.org/images/Biochar_book_Chapter_1.pdf., 2009.

[32] H.O. Pierson, *Handbook of Carbon, Graphite, Diamond, and Fullerenes*. Elsevier Inc Melbourne, 1993.

[33] M. Okamura, A. Takagaki, M. Toda, J.N. Kondo, K, Domen, T. Tatsumi, M. Hara & S. Hayashi, "Acid-Catalysed Reactions on Flexible Polycyclic Aromatic Carbon in Amorphous Carbon", *Chemistry of Materials*, 18, pp. 3039-3045, 2006. Doi. 10.1021/cm0605623.

[34] K. Nakajima, H. Michikazu & H. Shigenobu, "Environmentally Benign Production of Chemicals and Energy Using a Carbon-Based Strong Solid Acid". *Journal of the American Ceramic Society,* 90, 12, pp. 3725-3734, 2007. Doi.10.1111/j.1551-2916.2007.02082.x

[35] J.M. Thomas & W. Thomas, *Principles and Practice of Heterogeneous Catalysis,* Wiley-VCH, New York, 1997.

[36] Y. Wenzhi, A. Sultan, L. Klaus, G. Helena, Y. Wenzhi, A. Sultan, L. Klaus & G. Helena, "Noncovalent Functionalization of Graphene in Suspension", *ISRN Organic Chemistry,* pp. 1-7, 2013. Doi.10.1155/2013/656185.